THE SEISMOLOGICAL SOCIETY OF AMERICA
400 Evelyn Ave., Suite 201
Albany, CA 94706-1375
(510) 525-5474; FAX (510) 525-7204
www.seismosoc.org

Bulletin of the Seismological Society of America, Vol. 83, No. 2, pp. 416–435, April 1993

# THE 1912 ICELAND EARTHQUAKE RUPTURE: GROWTH AND DEVELOPMENT OF A NASCENT TRANSFORM SYSTEM

BY INGI TH. BJARNASON, PATIENCE COWIE, MARK H. ANDERS, LEONARDO SEEBER, AND CHRISTOPHER H. SCHOLZ

## ABSTRACT

**We have mapped in detail surface ruptures of the 1912 magnitude 7.0 strike-slip earthquake in south Iceland. This earthquake ruptured fresh basalt flows that had covered the pre-existing fault. The observed style of surface fracturing closely matches both theoretical predictions of the first stages of shear fracture development and microscopic-scale observations from laboratory experiments. The shear offset distributed across the zone of surface fractures produced by this earthquake is right-lateral and is in the range of 1 to 3 m. Total mapped rupture length is 9 km, but total rupture length is probably at least ~ 20 km. This interplate earthquake had an exceptionally high ratio of slip to fault length and, by inference, stress drop. The north-south trending rupture of the 1912 earthquake is part of the "bookshelf" faulting in the east-west trending South Iceland Seismic Zone. We ascribe the "bookshelf" faulting in the South Iceland Seismic Zone to a combination of the early development stage of the transform and regional strength anisotropy of the crust.**

## INTRODUCTION

Iceland is part of the Mid-Atlantic Ridge system, albeit an anomalous part. Icelandic crust is essentially of oceanic type, but it is at least three to four times thicker than normal oceanic crust (Bjarnason *et al.*, 1993). The crustal thickening is due to a hot spot centered under the east central part of the island. The excessive volcanism of the hot spot that feeds into the rift system has built up the thick Icelandic crust.

The North Atlantic rift system is moving WNW relative to the Icelandic hot spot (Morgan 1981; Vink, 1984). The rift system in the Iceland region has, however, followed the hot spot path by repeatedly jumping towards the east (Sæmundsson, 1974, 1979; Jóhannesson, 1980; Óskarsson *et al.*, 1985). As a result of these ridge jumps, the rift system in Iceland is offset 150 km from the offshore Reykjanes and Kolbeinsey Ridges (Fig. 1).

The rift system in Iceland is segmented into three parts, the Western, Eastern, and Northern Volcanic Zones (WVZ, EVZ, NVZ). An eastward ridge jump is thought to be in progress in south Iceland, where the young and southward propagating EVZ is taking over the crustal spreading of the older WVZ (Pálmason and Sæmundsson, 1974; Einarsson and Eiríksson, 1982). Fracture zones are developing to accommodate transform motion between the eastward offset of the Icelandic rift system from the Reykjanes and Kolbeinsey Ridges: The Tjörnes Fracture Zone in the north and the South Iceland Seismic Zone (SISZ) in the south.

The SISZ was identified as an east-west–striking left-lateral transform zone based on its geometrical relationship with the ridge system and one fault plane solution that shows strike-slip faulting on an east-west or a north-south–striking plane (Stefánsson, 1967; Ward, 1971). Transform motion between the

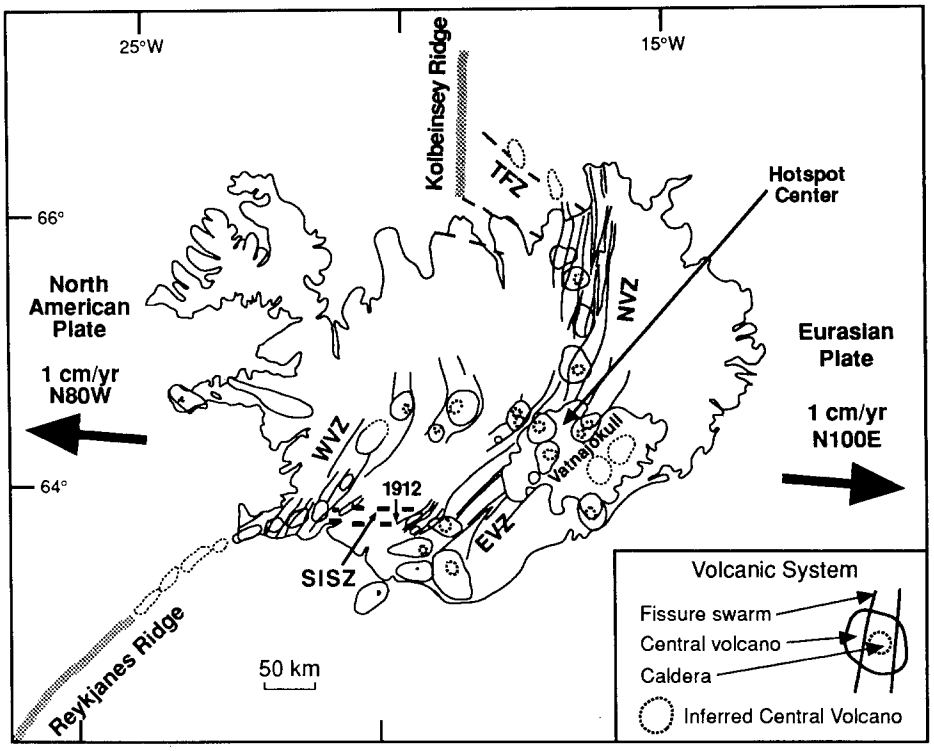


FIG. 1. Tectonic and volcanic features of Iceland. The Eastern, Western and Northern Volcanic Zones (WVZ, EVZ, NVZ) are delineated by chains of volcanos and rift zones. The South Iceland Seismic Zone (SISZ) connects the Eastern Volcanic Zone with the spreading centers on the Reykjanes Peninsula. The Tjörnes Fracture Zone (TFZ) offsets the Northern Volcanic Zone from the Kolbeinsey Ridge. The epicenter of the 1912 earthquake is indicated. (Figure modified from Einarsson and Sæmundsson (1987) and Hackman *et al.* (1990).

EVZ and the Reykjanes Ridge is taken up along the SISZ and continuous into the WVZ along the Reykjanes Peninsula as inferred by focal mechanisms (Einarsson, 1991; Fig. 2). The SISZ extends over an area 60 to 70 km long and 10 to 15 km wide in the populated South Iceland Lowlands between the overlapping WVZ and EVZ. Large destructive earthquakes, with magnitudes up to 7.0, have occurred in the SISZ throughout the 1100 years history of settlement in Iceland (Einarsson *et al.*, 1981; Halldórsson *et al.*, 1984). Major earthquake sequences in which most of the zone is affected tend to last from a few days to a few years. The sequences occur at average intervals of 80 to 100 years. Each sequence typically begins with a magnitude 7 earthquake in the eastern part of the zone, followed by smaller events farther west. The last sequences occurred in 1732 to 1734, 1784, and 1896, so the next sequence is expected soon (Einarsson, 1985). Single large events that are not part of a major sequence also occur. These events are located near the eastern or western ends of the zone and include the magnitude 7.0 earthquake west of Hekla in 1912 (Figs. 1 and 2).

East-west faults have not been identified from surface mapping along the SISZ. Instead historic earthquakes are known to have north-south elongated damage areas and to have produced north-south–striking surface ruptures (Einarsson *et al.*, 1981; Einarsson and Eiríksson, 1982; Fig. 2). These surface

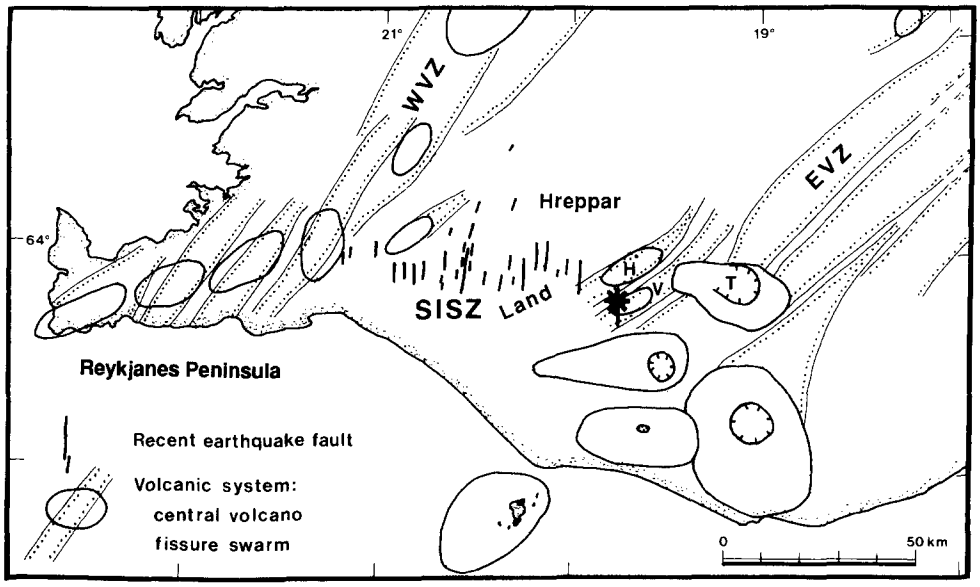


FIG. 2. Tectonic index map of south Iceland. The South Iceland Seismic Zone (SISZ) consists of a series of north-south striking faults (solid lines). The Hekla, Vatnafjöll, and Torfajökull central volcanos are marked as H, V, and T, respectively. The epicenter of the 1987 Vatnafjöll earthquake is marked with a star. The easternmost fault west of Hekla ruptured in the 1912 earthquake. Recent earthquake faults and volcanic systems are from Einarsson and Sæmundsson (1987).

ruptures have been traced up to 10 km and are characterized by northerly trending arrays of en-echelon fractures that are dominated by opening mode displacements. We refer to these as tension fractures; in between them are compressional pushups. This type of en-echelon fracture pattern has been observed before in soil layers covering a fault (e.g., Tsuneiski *et al.*, 1978), but in Iceland and Hawaii (Jackson *et al.*, 1992) the fractures are observed in hard rock (mainly basalt) as well as soil. The individual tension fractures in the SISZ normally strike 30° to 40° to the east of north, indicating overall right-lateral movement within the shear zone.

This style of faulting is theoretically predicted for the first stages of shear fracture development and has been observed at the microscopic scale in laboratory experiments (Cox and Scholz, 1988). The shear fractures form in the Coulomb orientation, but they originate from a coalescence of tensile cracks that align individually in the direction of maximum principal stress (e.g., Lawn and Wilshaw, 1975; Paterson, 1978; Cox and Scholz, 1988; Scholz, 1989). As slip accumulates, it becomes localized on a single plane, the plane with the Coulomb orientation. The surface observations of faults in the SISZ indicate that they are in the this first stage of fault development. At depth they may be more fully developed.

The overall east-west left-lateral transform motion along the SISZ appears to be accommodated by right-lateral motion on many parallel transverse faults distributed along the zone. This type of faulting has been called "bookshelf" faulting. Hackman *et al.* (1990) concluded that the east-west transform motion on the SISZ could be accommodated by bookshelf faulting, if the north-south faults are longer or spatially more frequent than currently mapped. Einarsson

and Eiríksson (1982) speculated that the transform zone is migrating southward with the propagation of the EVZ and that net displacement has not been enough to break the whole crust in a major through going east-west transform.

The 1987 Vatnafjöll earthquake is the largest earthquake ($M_w$ = 5.9) in south Iceland since the 1912 magnitude 7 earthquake and was the first event sufficiently large to allow a meaningful study of source processes in this region (Fig. 2 in Bjarnason and Einarsson, 1991). It occurred in the EVZ, in a direct continuation of the SISZ. The earthquake was associated with right-lateral strike slip faulting on a north-south–striking vertical fault plane. It resembled the large historic earthquakes in the SISZ and shows that the transform zone extends further into the rift zone than previously recognized. The earthquake ruptured an approximately 10-km-long fault in the lower crust down to 15-km depth. We infer from the subsurface rupture pattern of the Vatnafjöll earthquake and the many north-south surface ruptures of large historical SISZ earthquakes that these events represent north-south right-lateral ruptures through the whole seismographic layer. Based on the estimated maximum magnitude of 7, thickness of the seismogenic layer of 10 to 15 km, and 10- to 15-km fault length, it follows that large SISZ earthquakes should have an exceptionally high ratio of slip to fault length and high stress drops.

Prior to this work only one direct field measurement of fault slip existed for strike-slip faults in SISZ, a 0.8-m slip measured at the southern end of the 1896 surface rupture in the Land district (Einarsson and Eiríksson, 1982; Fig. 2). One of the main objective of this work was to collect more slip data from the seismic ruptures within the SISZ to investigate the slip to fault-length ratio. Another objective was to map in greater detail than before the very unique surface rupture patterns of the SISZ earthquakes, which is relevant for understanding early fault development.

## Fault Observations

We focused this study on the surface rupture of the magnitude 7.0 earthquake that occurred in 1912 at the eastern end of the SISZ. This earthquake has one of the best preserved surface ruptures in the SISZ and is the only large earthquake in the area with an instrumentally determined magnitude (Kárnik, 1969).

The most characteristic feature of the 1912 surface rupture, as well as other strike-slip faults in the SISZ, is the en-echelon arrangement of fractures at a wide range of scales (Einarsson and Eiríksson, 1982). At the largest scale, the 1912 fault zone can be described as a north-south–striking array of at least eight northeasterly trending fault segments (Fig. 3). The lengths of most of the fault segments are not clearly defined but they are at least several hundred meters to about a kilometer long. The six most westerly fault segments define the main fault zone striking north-south. They are arranged in a relatively narrow en-echelon array, approximately 600 m wide and 9 km long. The fault segments are inclined on average 15° clockwise from the overall north-south strike of the fault zone. The two most easterly segments are splay faults of the main fault. The one going up the polagonite ridge Bjólfell is newly reported in this work.

The fault segments can be subdivided into "arrays of tension fractures" (Fig. 4a). Each array is typically tens of meters long and is rotated on average 20° in a clockwise sense from the north-south strike of the fault zone (Fig. 4b).

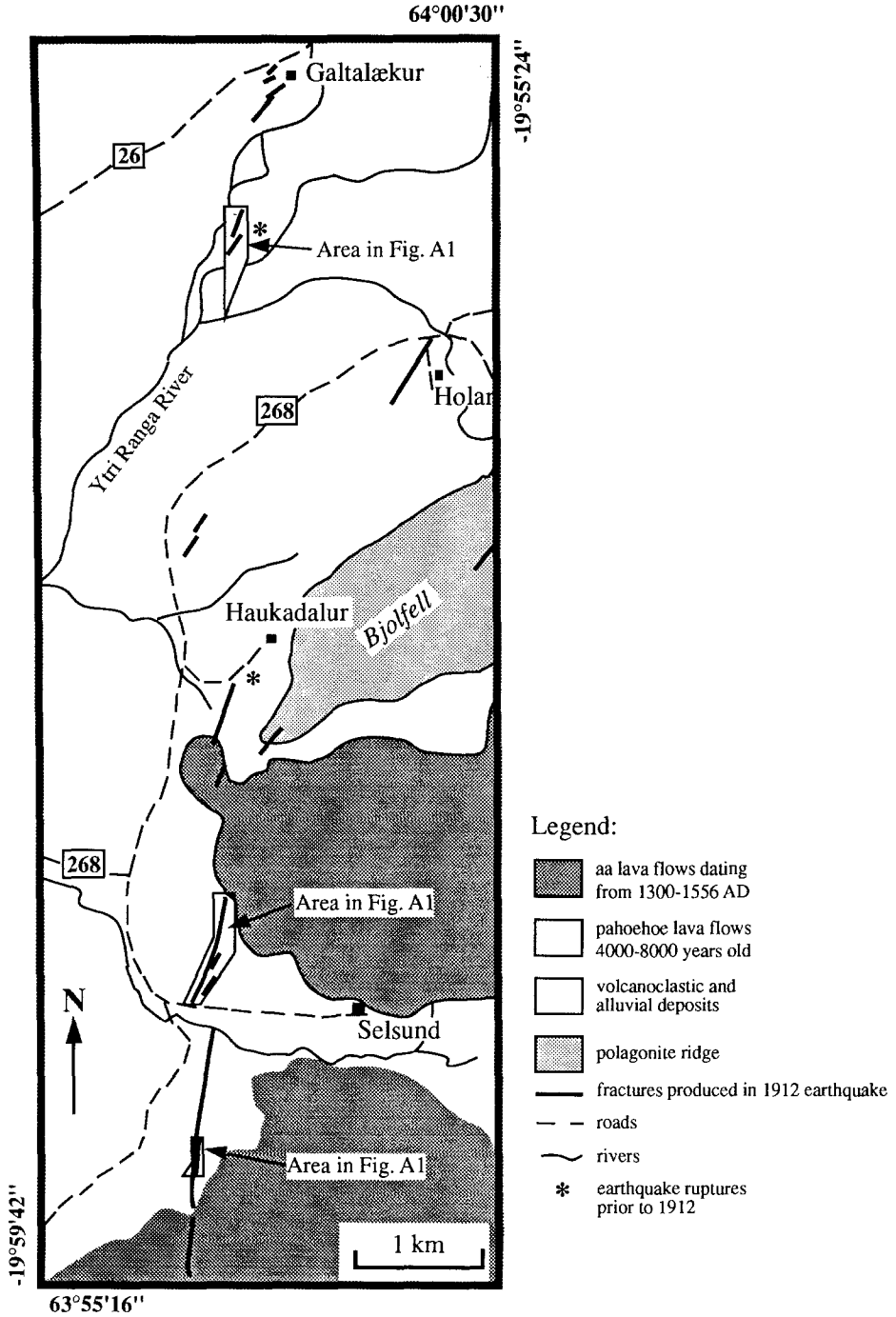


FIG. 3. Map of surface ruptures of the 1912 earthquake.

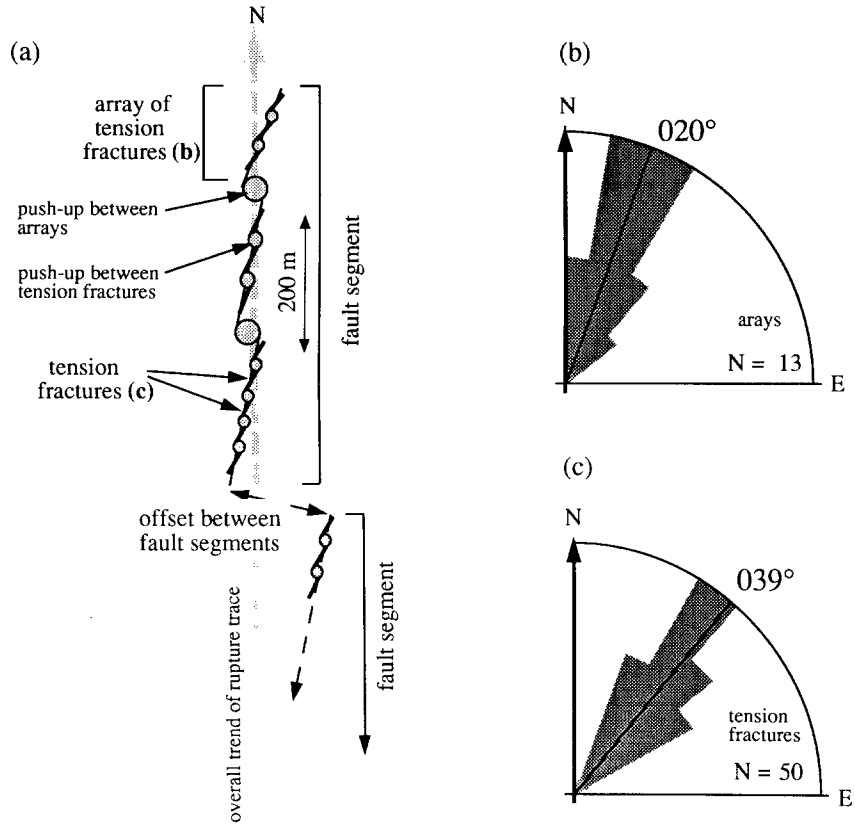


FIG. 4. (a) Schematic diagram showing the en-echelon components of the 1912 rupture. (b) Orientation of tension fracture arrays as determined from field measurements (mean orientation N20°E). (c) Orientation of individual tension fractures as determined from field measurements (mean orientation N39°E).

On the smallest scale, documented in this work, are the tension fractures themselves that make up these arrays. The tension fractures are on the order of meters in length with mean orientation approximately N40°E (Fig. 4c). This pattern of left-stepping en-echelon fractures is consistent with right-lateral shearing in a north-south fault zone. The left-stepping is on the order of several hundred meters between the fault segments, tens of meters between the "arrays of tension fractures," and meters between the individual tension fractures.

Between the ends of the arrays and individual tension fractures are compressional push-up structures, where the lava flows have been domed up during the rupture process (Fig. 4a). These structures are created by buckling of the topmost lava flow or, in some cases, by thrusting up of the topmost sheet of lava.

The best preserved portions of the 1912 surface rupture are in the pahoehoe lava flows with little or no soil cover. In places of alluvial sediments or in places of aa lava flows, the surface rupture has been covered and cannot be traced with any confidence. The currently mapped surface rupture of the 1912 earthquake is therefore rather unlikely to be complete.

We chose to map in greater detail ($\sim$ 0.5 m) than had been done before (Einarsson and Eiríksson, 1982) the surface rupture of the 1912 earthquake at three of the best exposed fault segments. The maps were created using a Zeiss Elta 4 tachometer, a surveying instrument that allows a chosen point to be

assigned $(x, y, z)$ coordinates relative to a reference point. This technique allowed us to create accurate maps of features as small as a few tens of centimeters. The limitation on the size of the smallest feature that could be resolved was generally determined by the preservation of the outcrops not the resolution of the mapping technique. The orientation of the maps with respect to true north was obtained by a compass with a few degrees accuracy.

Below are descriptions of the maps from three locations where the rupture is exposed from north to south along the fault.

*Fault Segment: Galtalækur*

The Galtalækur site is located between the Ytri-Rangá (river) to the east and one of its tributaries to the west (Fig. 3). The cliffs exposed along these two rivers offer the only opportunities for examining the shallow subsurface structures close to the trace of the rupture. These exposures show that the surface lava flow is 2 to 4 m thick and rests on an unlithified layer of volcanoclastic material, which is presumably much weaker than the overlying lava layer.

The northernmost exposure of the rupture that we mapped is 1 km SSW of the farm Galtalækur (Fig. 3). At this location there are two subparallel, northeasterly striking "arrays of tension fractures" (Figs. 5 and A1). The northern most of these arrays can be traced for a distance of 300 m until it dies out at its northern end. The southern most array is 175 m long and is truncated by a steep cliff at its southern end. The two arrays overlap by 30 m and are offset in a left-stepping fashion by a distance of approximately 60 m. The array to the north is exposed in the bare 7.8- to 8.2-ka-old Thjórsá pahoehoe lava flow (Olsson *et al.*, 1967, Hjartarson, 1988), whereas to the south the lava flow is covered by a layer of soil approximately 5 m thick. In general, the rupture structures at this locality are not arranged in as regular a pattern as at some other places along the fault.

The northern array has a trend varying between N45°E at its northern end to approximately due north at its southern end, where it curves into the southern array. A region approximately 40 m wide and 70 m long has subsided between the two arrays. The fractures along the northern segment are not simple opening mode tensile cracks, but also exhibit considerable shear. A direct slip measurement was possible on one of these fractures, giving a slip vector of 1.0 m with a trend of N20°E and plunge 10°.

The push-ups are formed by buckling or thrusting of the topmost lava flow, often with only a rough sense of vergence discernible (see inset of Fig. 5). The largest push-up at this locality (2.2 m in height) occurs at the southern end of the northern segment and is formed by thrusting of the lava towards the northeast. This push-up is elongated trending N40°W.

The south array is exposed on a 5-m-thick loess bench that overlies the lava flow. Here it was not possible to get direct measurements of the opening of the tension fractures due to the soil cover, but the general outlines of the tension fractures are visible as deep holes in the soil. No evidence was found of the rupture in the cliff section along the Ytri-Rangá although the fault trace extends very close to the edge of the cliff (Fig. A1).

*Fault Segment: Haukadalur*

In the area of the Haukadalur farm, faulting associated with the 1912 earthquake is multi-stranded on the large scale (Fig. 3). The farmer at

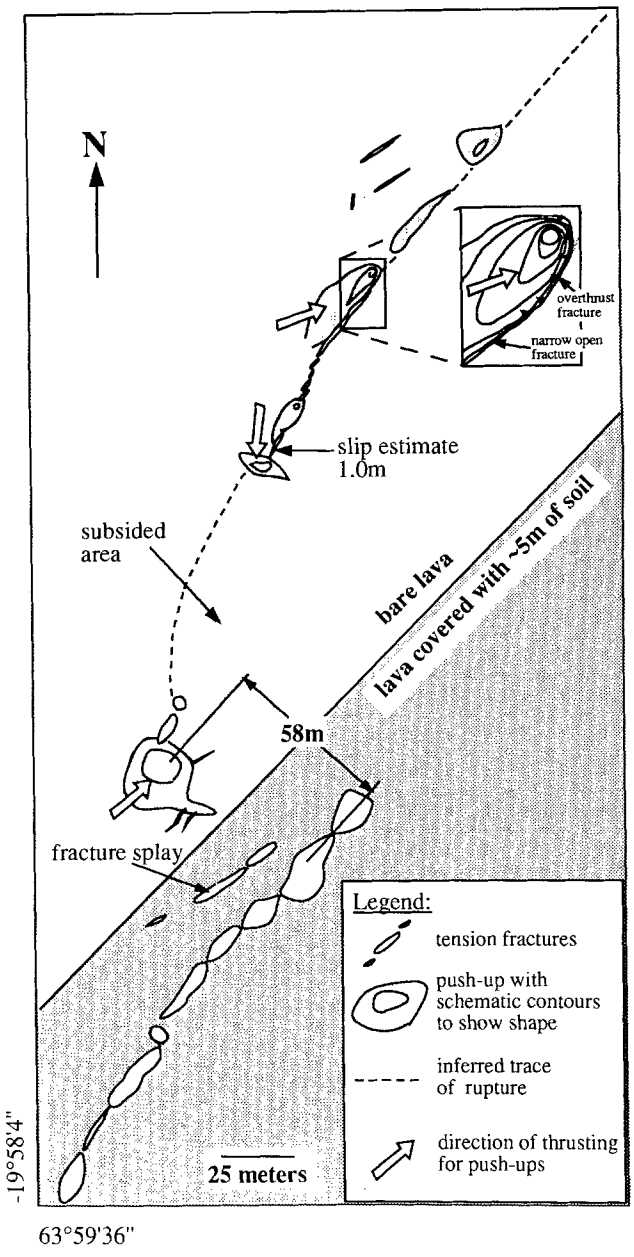


FIG. 5. Map of the rupture trace at Galtalækur. Inset shows details of a push-up.

Haukadalur Mr. Magnús Runólfsson (1900–1991) told us that one of the surface ruptures associated with the event, could be traced along the southern crest of the Bjólfell polagonite ridge. According to his account, much of this trace had been obliterated by subsequent road work. We walked the entire 2.5-km-long ridge and found fissures over most of its length, except for the portion that had been effected by road work.

The Bjólfell ridge is generally very sharp topographically. Such a topography is apt to cause large amplification of seismic waves. Thus, it is possible that

fissuring along the ridge may have been induced by particularly strong shaking in 1912. Along the high and topographically sharp portion of the ridge, left-stepping en-chelon fracture sets and local right-lateral displacement on single fractures was observed. Generally, however, the pattern of fractures appeared to be chaotic, and the case for faulting would be weak if based only on the fractures along the high ridge. In contrast, the southernmost portion of the ridge is characterized by a broad topographic profile where topographic amplification effects would probably have been subtle. A very regular pattern of en-echelon fractures consistent with right-lateral faulting was found in this portion of the ridge. These fractures can be followed to the south to within 0.5 km of the previously known trace of the 1912 event.

Considering the rather continuous pattern of fracturing along the ridge, the evidence for right-lateral displacement along the southern portion of the ridge and the eyewitness account that these features were formed in 1912, we conclude that they represent a branch of the fault system that ruptured in 1912. This fault is clearly correlated with the ridge and by implication, with the dike or fissure that erupted during glaciation in the upper Pleistocene (Jóhannesson *et al.*, 1990). A young dike is probably associated with a thermal anomaly that would tend to locally weaken the rock. Thus, a dike may represent a pre-existing weakness and a likely place for a fault to develop. All the major Mesozoic dikes that cut across the Appalachians in the vicinity of the Gettysburg Basin in northeast America coincide with faults (Leonardo Seeber, work in progress).

*Fault Segment: Selsund North*

The largest rupture structures and the most regular en-echelon pattern of the 1912 rupture are on the fault segment to the northwest of the Selsund farm (Fig. 3). Here the rupture is very well exposed in a pahoehoe lava flow covered by a thin (< 50 cm) soil layer. In this locality, the rupture trace consists of a fault segment that trends approximately N19°E and has a total length of at least 900 m. The trace of the fault is lost in the younger and rougher aa lava flow to the north. The central part of this fault segment (Fig. 6) has two subparallel fracture strands. It can be inferred from the sizes of the tension fractures that the western strand took up the majority of the slip. Push-ups reach 2.3 to 2.6 m in height and tension fractures reach up to 15 to 20 m in length on this fault segment. Two ponds were formed along the rupture trace at this locality by water accumulating in topographic depressions created by the 1912 earthquake (Figs. 6 and A1). Although we were unable to make a direct measurement of slip, we believe the largest surface displacement occurred on this segment, based on the relative sizes of rupture structures.

Two minor sets of tension fracture arrays with easterly trends at this locality exhibit a right-stepping en-echelon pattern that is consistent with left-lateral shearing (Fig. 6).

*Fault Segment: Selsund South*

Southwest of the Selsund farm another segment of the 1912 rupture is exposed in pahoehoe lava (Figs. 7 and A1). The fault segment is composed of two strands, separated by up to 40 m. It can be inferred from the sizes of the tension fractures that most of the slip is taken up by the western strand. The soil layer sometimes obscures the detail of the rupture on this segment, but usually the pattern of en-echelon tension fractures are reflected by linear depressions where

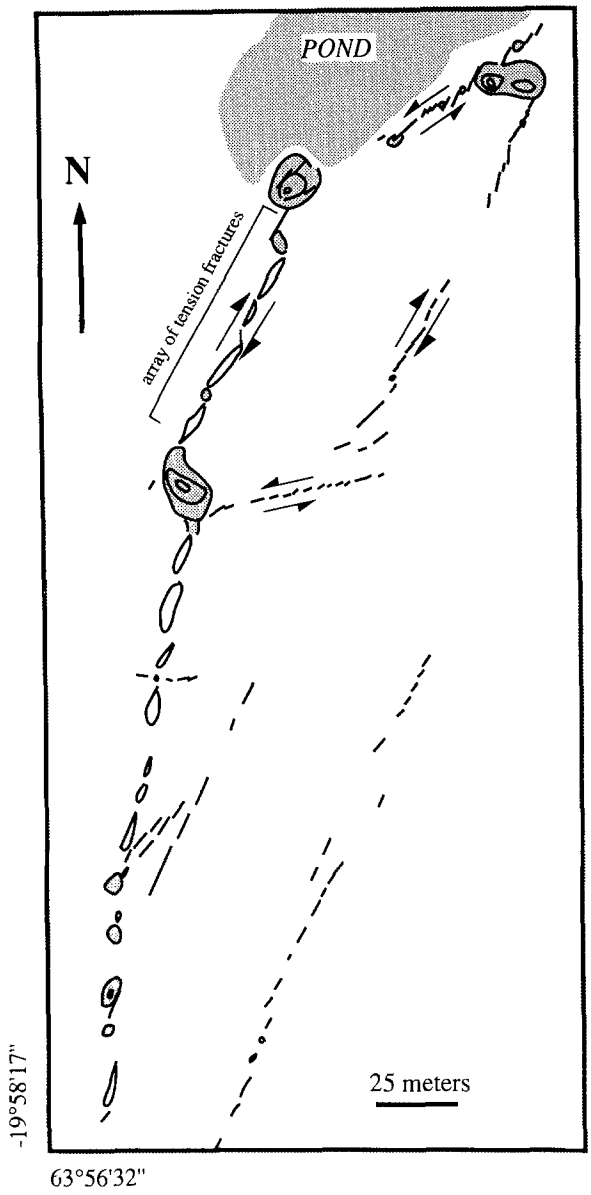


FIG. 6. Map of the rupture trace at Selsund North (see Fig. 5 for legend). Arrows indicate sense of motion inferred from tension fractures.

the vegetation has subsided into spaces created in the lava beneath. A hole, almost circular in shape with a diameter of 2 to 3 m, is exposed along the eastern strand (Fig. 7). The hole is partially filled with medium-size pumice and sand. We determined this structure to be a "blow hole" caused by liquefaction of saturated sand during the 1912 earthquake.

A total slip of 3 m during the 1912 earthquake was determined for this fault segment, using the offset of deeply worn sheep tracks crossing the two strands of the rupture trace. It was possible to make indirect estimates of surface slip in other places along the fault, which we describe below.

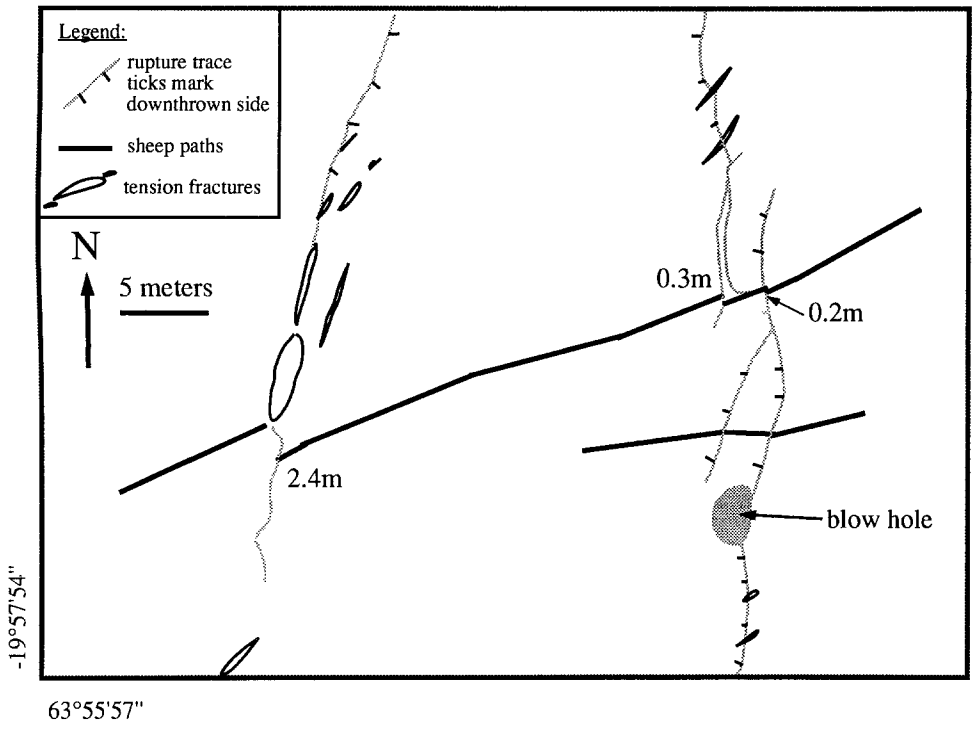


FIG. 7. Sheep paths, offset by a total of 3 m, used to infer surface slip at the Selsund South rupture trace.

*Estimates of Shear Offset*

In general, direct measurements of the total shear offset across a fault zone is difficult to make. We were able to measure the total distributed shear offset across the 1912 rupture zone at only one place: 3 m on the Selsund South segment. The deformation on the surface of the 1912 rupture is complicated and contains components of compression, extension, and rotation as well as shear. The dimensions of the push-ups along the rupture trace give a measure of the compressional component of the rupture field that may be related to the shear in the zone as shown below. The calculated shear offset will be a minimum, because it is based on only a measure of the compressional component of the deformation field. Even the calculations of the compressional component within the shear zone are underestimated because the sagging of the push-ups, since their creation (which has been observed by the local people) are not taken into account.

Figure 8a shows an idealized push-up within a strike-slip shear zone. We assume that the short axis of a push-up forms at 45° to the maximum shear direction and that the height $h$ and the diameter $d_r$ of the push-up are related in a simple way to the amount of shortening. For a two-dimensional push-up (Fig. 8b), triangular in cross section, the amount of shortening $s$ is given by:

$$s = d_r(1/\cos\phi - 1), \tag{1}$$

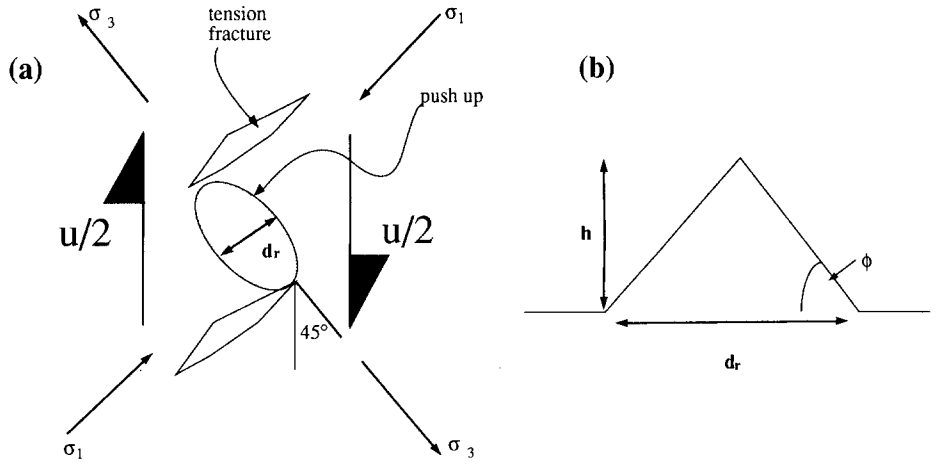


FIG. 8. (a) Schematic diagram showing orientation of a push-up, tension fractures, principal strain axes, and shear offset vectors. (b) Push-up in cross section. See text for discussion.

where $d_r$ is the short-axis diameter of the push-up and $\cos \phi = d_r / \sqrt{(4h^2 + d_r^2)}$. The amount of shear offset $u$ on the fault is given by

$$u = s/\cos 45°. \tag{2}$$

The amount of surface slip near Galtalækur was calculated to be between 0.4 and 0.6 m based on the dimensions of the push-ups. A direct shear offset measurement of 1.0 m was made at this locality. This number is, however, a minimum shear estimate, because the total shear over the fault zone is distributed over a wider area than the width of a tension fracture where the measurement was taken. On the Selsund North segment, the maximum slip determined from the two largest push-ups was calculated to be 1.25 m. This compares to the direct total slip measurement of 3 m on the Selsund South segment, which probably had less slip than the Selsund North segment (based on the sizes of push-ups and tension fractures).

*Fault Length*

We interviewed two Icelandic farmers, Mrs. Jónína Haflidadóttir (b. 1902) and Mr. Magnús Runólfsson (1900–1991), that lived at the Haukadalur farm, which is near the mapped ruptures (Fig. 3). At the time of the 1912 earthquake Jónína lived on the Foss farm. She reported that she saw surface ruptures in Árholt, extending both to the north and southward to the northern bank of the Eystri-Rangá (river), about 12 km south of the mapped end of the fault. Magnús reported that, while he had not personally seen the ruptures in Árholt, he had spoken with several other people from the area who had. He had also personally traced the rupture 1.5 km south of the mapped southern end, to Fálkhamar. Both of these farmers were well acquainted with the 1912 ruptures in the Haukadalur region and reported that the others that they had seen in 1912 and later had the same character. These ruptures may be difficult to find today, because a large part of that area is covered with sand and aa lava flows. We accept this eyewitness evidence and conclude that rupture extended 12 km

south of the mapped end of the fault. It is probable that the rupture extended a few kilometers further to the north than currently mapped. However, interviews with several persons gave conflicting evidence on this account. We conclude that the total rupture length on the fault was approximately 20 km in the 1912 earthquake.

*Older Earthquake Ruptures*

We found evidence of older surface rupture(s) along the 1912 fault. Linear depressions in the soil bench, near the Galtalækur segment (Fig. 3) probably represent soil filled tension fractures formed in an older earthquake. They have the same strike as the tension fractures of the 1912 earthquake, but are offset 100 to 150 m to the east. The soil bench has a flat surface, which makes the depressions very distinct, with dimensions on the order of 10 to 20 m long, 5 to 10 m wide, and 1 to 2 m deep. The depressions are fully grown over with approximately 15° steep slopes, whereas the 1912 rupture of the same soil layer appear as deep holes with approximately 50° steep slopes.

We excavated down to approximately half the depth of the soil bench in one of these depressions, to establish the age of the older rupture event. The soil bench is approximately 5 m thick and sits on top of the Thjórsár basalt lava flow. The soil is mostly composed of loess and volcanic ash. The ashes comprise about 25% of the soil volume. Most of the ash units are derived from eruptions of the central volcanos Hekla and Katla. In the trench we encountered 21 measurable ash horizons (Fig. 9). None of the ash horizons were disturbed, indicating that the second event was older than the 3.5-ka age assigned to the lowest ash horizon. That age is based on a correlation of the layer to the Selsund ash, which has been dated at about 3.5 ka (Gudrún Larsen and Bryndís Róbertsdóttir, personal comm., 1992). We did not observe step-like offsets of ash horizons in the trench similar to those observed on the side walls of the 1912 soil gashes. Deeper excavation was prevented because of a lack of available shoring for the 3-m-deep hand-dug trench.

Ash layers exposed in the trench (Fig. 9) show no thickening down slope. It could be argued that the lack of down slope thickening could be interpreted as the result of a partial opening in the basalt horizon (possibly in the 1912 earthquake), which did not break through to the surface. The subsequent draping of overlying sediment would result in a smooth appearance similar to what is observed. The lack of down-slope thickening was somewhat surprising, since we expected that such a large depression would result in sediment accumulation, as wind-blown or water-lain ash is trapped at the bottom of the depression. The difficulty with this argument is that the post-1912 ash horizons also show no thickening. The 1970 Hekla eruption produced a thin ash layer found within the Galtalækur area that is visible in the uppermost portion of the trench. Here, the ash is deposited in and overgrown by a thick matting of grass. It is our reasoning that a thin ($< 1$ to 2 cm) ash fall would be trapped by the grass and thereby not transported down slope. Thicker ash horizons ($> 2$ cm) like the 900 AD settlement layer (L in Fig. 9) have variable thicknesses. We suggest that for thicker ash falls the grass is quickly buried and subsequently surface material is more easily transported, causing the observed variable thickness.

Another argument against the origin of the depression being a collapse structure of the 1912 earthquake is the lack of extension faults or any breaks or

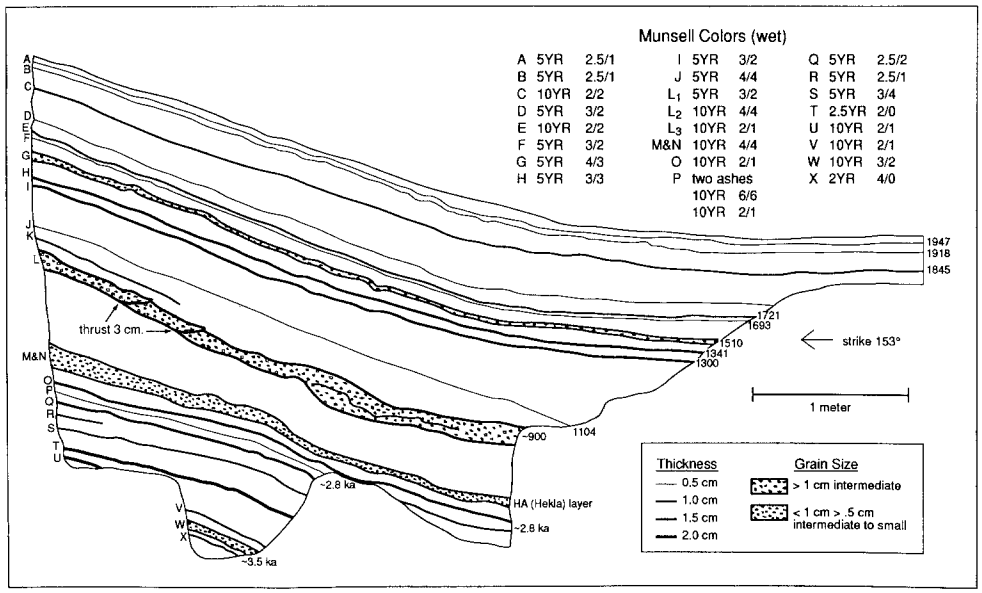


FIG. 9. Map of trench wall from pre-1912 tension fracture located 1.4 km SSW of the Galtalækur farm (Fig. 3). Orientation of the trench was N53°W and the total depth was 3 m. Lines represent ash layers from eruptions of the central volcanos Hekla and Katla. Assignment of historical dates is based on a correlation with the Galtalækur section 22 from Fig. 3 in Thórarinsson (1967) and prehistoric ages are from Larsen and Róbertsdóttir (personal comm., 1992). Line thickness is proportional to the thickness of the measured ash horizons. Ash color is assigned using the Munsell soil color chart. Open circles represent a grain size of between 1 and 2 cm. Dark circles represent grain size of less than 1 cm. No horizons were found to be offset. Thicker horizons showed some variability in thickness that was not reflected in underlying thinner horizons, indicating that variations in thickness are not due to tectonics.

stretching in the ash horizons. Such structures would be expected for a horizon that would have been dropped over 1 m in the 1912 event. Moreover, the thickest horizon (layer L) has two small 3-cm-long downward-directed thrust faults. The trusts sole into the "L" ash horizon and cannot be traced into horizons above or below. These thrust structures are consistent with what might be produced by a small gravity-driven surface slump.

These arguments suggest that the depression was formed sometime before 3500 years ago. The lack of broken ash surfaces leaves the possibility that something other than an earthquake caused the depression. However, the similarity in trend and aspect ratio of the overgrown depressions to the trend and aspect ratio of the 1912 ruptures, combined with the lack of other depressions on the otherwise uniformly-flat loess bench, suggest to us that this depression was caused by an earlier earthquake rupture event.

Further evidence of an older surface rupture was found in a finiglacial sand-stone layer near the Haukadalur farm and approximately 150 m east of the 1912 fault segment at this place (Fig. 3). A brecciated zone approximately 0.5 m wide trending N30°E is exposed in the sandstone. Two conjugate sets of fractures and joints occur in the brecciated zone. One set strikes approximately N20°E and the second set strikes between N50°E and 75°E. A small scale ($< 5$ cm) right-lateral shear was observed on some of the fractures striking N20°E and left-lateral shear on some fractures in the conjugate set, consistent with right-lateral shear on this fault. The sandstone is about 10 ka old (Helgi Torfason, personal comm., 1992).

The Thjórsár lava flow that was offset by the 1912 earthquake is dated with C14 between 7.8 to 8.2 ka (Olsson *et al.*, 1967; Hjartarson, 1988). The undisturbed ash horizons encountered in the excavated trench at 3-m depth is 3.5 ka old. We therefore conclude that the older rupture occurred between 8 and 3.5 ka. Evidence of this same rupture or a third rupture that predates the 1912 rupture was found in the 10-ka finiglacial sand-stone layer near the farm Haukadalur as described above.

The Thjórsár lava covers a large part of the study area. An extensive air photo and ground reconnaissance of the Thjórsár lava flow found no evidence of another rupture younger than 8 ka. We infer that two surface ruptures occurred in 8 ka.

## Development of Faulting in the SISZ

The right lateral faults in the SISZ appear to represent the nascent stages of a transform zone connecting the EVZ and the Reykjanes Ridge in southwestern Iceland. Understanding of this fault system is still incomplete. Einarsson and Eiríksson (1982) suggest that the SISZ is a migrating fracture front moving southwards in response to the propagating EVZ. Therefore they argue that the transform zone has not had enough total displacement to break the whole crust in a major east-west transform fault. One of the most curious yet unexplained features of the SISZ is the formation of bookshelf faulting during the nascent stage of the transform.

A partial explanation for the formation of these bookshelf faults may lie in pre-existing planes of weaknesses as controlling factors in their formation. In the area of the SISZ, recent lava flows, vegetation, and river and glacial outwash cover many such pre-existing structures. However, in the Hreppar district to the north of the SISZ, there is an excellent exposure of late Tertiary rock (Jóhannesson *et al.*, 1990), which may typify such observed pre-existing structures. The rocks show abundance of normal faults with rather small variance around an average strike of N36°E (Fig. 10). The normal fault fabric and planes of weaknesses associated with volcanic dikes were created by the crustal extension associated with the rifting and are approximately parallel to the EVZ and WVZ. This general trend of pre-existing structural trend can be safely extrapolated to and beyond the SISZ in south Iceland. Superimposed on these rifting structures are a number of north-south–trending fractures, for which at present the style of faulting has not been determined. If the SISZ is a migrating transform, then presumably the north-south fractures could be older

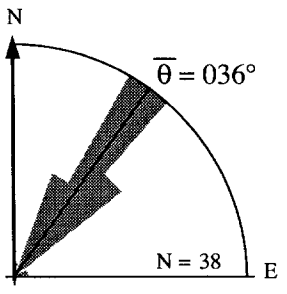


FIG. 10. Orientation of ridge generated normal faults in the Hreppar district as determined from geological map (Jóhannesson *et al.*, 1990) (mean orientation N36°E).

strike-slip faults created by the transform when it was located further to the north.

We hypothesize that the north-south trend of the strike-slip faults in the SISZ is due to the orientation of the pre-existing structural trend in the area that introduces a strength anisotropy in the crust. Based on the east-west trend of the SISZ and the north-south strike-slip faults, one can infer a stress field with vertical planes of maximum shear stress striking approximately north-south and east-west. As the general trend of the pre-existing structures in the area is closer in direction to the north-south maximum shear stress plane than the east-west plane, the crust is weaker in that direction. Shearing along a north-south direction could therefore be achieved more easily by transferring a slip over a set of pre-existing northerly striking planes of weakness, whereas shearing along an east-west direction would involve breaking through a larger percentage of unfractured material (Fig. 11). The variation in the strike direction of the fault segments of the 1912 rupture could, for example, be explained by slip on a number of pre-existing planes with slightly different orientations.

A second hypothesis for the north-south fracture orientation in the SISZ is reactivation of normal faults that have rotated approximately 36° to their present north-south direction, due to the east-west left-lateral displacement in the area. Difficulties with this hypothesis are the following: (1) We assume that the zone was broken up into blocks of 3 km wide and 15 km long, with the long sides as reactivated normal faults striking N36°E. These dimensions are based on the 15 km width of the SISZ and approximately 3 km spacing of the mapped north-south fractures in the zone. The reactivated normal faults would then need to take up a total of 2.1 km accumulated shear offset to achieve a rotation of N36°E. For narrower blocks, say 1 km wide, the accumulated shear offset would be 700 m. There is no morphological evidence for such large displacements. (2) A geometrical argument can also be made against this hypothesis. Let us assume that the north-south fractures in the Hreppar district are older strike-slip faults created in the same way as the younger currently active strike-slip faults in the SISZ. The north-south fractures are superimposed on many of the N36°E striking normal faults. This would clearly be impossible within the framework of the blocks that have rotated 36°.

The pattern of en-echelon tension fractures that characterizes the 1912 rupture trace is very similar to the fracturing produced at the tip of a propagating Mode III shear crack in controlled laboratory experiments (Cox and Scholz, 1988). In these experiments, an array of oblique tensile cracks forms just in

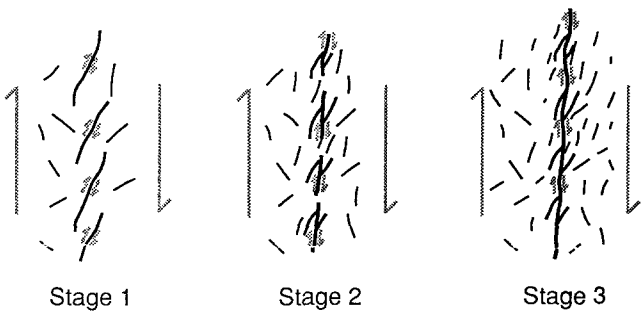


FIG. 11. Schematic diagram showing stages of progressive evolution of north-south strike-slip faults by reactivation of pre-existing normal fault fabric.

front of a starter notch that is loaded under shear. The tensile cracks gradually become linked together by additional oblique fractures to form a macroscopic shear fracture as deformation proceeds. Eventually a through-going slip surface is formed surrounded by a zone of irregular fracturing called a "brittle process zone." By analogy, the surface rupture pattern of the 1912 earthquake represents the Mode III edge of a strike-slip fault propagating up towards the surface. The en-echelon pattern of tension fractures corresponds to the T-fractures observed by Cox and Scholz (1988). At depth the fault that the 1912 earthquake occurred on must be more developed. Fault scaling studies find that displacement-length ratio of $1.0 \times 10^{-2}$ is expected for most faults (Cowie and Scholz, 1992). The fault of the 1912 earthquake has therefore probably accumulated the order of 200 m at depth. At the surface, the fault is repeatedly buried by basalt flows originating from the EVZ. In 1912, the fault ruptured through at least one of these surface flows at places where it had not ruptured before. Repeated slip along the same zone would destroy the delicate fracture pattern observed today and concentrate the deformation to ultimately produce a through-going fault. However, due to the proximity of the fault to the active EVZ, it is very likely that it will be resurfaced with lava and that new fresh "brittle process zone" will be created in a future earthquake.

The two direct shear offset measurements give a 1.0-m minimum shear offset at the northern end and a 3-m total distributed shear offset at the southern end of the mapped fault trace. As mentioned above, the southern end of the mapped fault trace may actually be close to the center of the entire fault. The calculated slip estimates are in the range of 0.4–1.25 m, which are likely underestimates. In spite of these limited measurements, we think it is reasonable to assume an average slip of $\sim$ 2 m along the fault.

The co-seismic average slip on the fault can be estimated by using the Hanks and Kanamori (1979) moment-magnitude relation together with the moment relation $M_0 = \mu \Delta u S$, where $\mu$ is the shear modulus, $\Delta u$ is the average slip, and $S$ the fault area. The 1912 earthquake had an estimated surface-wave magnitude of 7.0 (see Appendix B) and a rupture length of 20 km, and ruptured from a depth of 15 km (which is the maximum rupture depth of the Vatnafjöll earthquake (Bjarnason and Einarsson, 1991)) to the surface. We obtain an average co-seismic slip of 3.3 m. A second method of estimating slip uses the Gutenberg-Richter empirical energy relation (see Bjarnason and Einarsson (1991)). This method gives a slightly lower value of 2.4 m. These numbers agree well with the estimated average surface slip of $\sim$ 2 m.

These slip estimates give considerably larger ratio of slip to fault length, $\sim 1 \times 10^{-4}$, than the average ratio of $1 \times 10^{-5}$ for interplate earthquakes (Scholz *et al.*, 1986). The ratio is even higher than the ratio for intraplate earthquakes of $6 \times 10^{-5}$, as found by Scholz *et al.* (1986). Since stress drop scales linearly with the ratio of slip to fault length, we infer that the 1912 earthquake had a high stress drop, indicating a "strong" fault. The 1912 earthquake is similar to other large SISZ historic earthquakes, so we conclude that the north-south strike-slip faults in the SISZ are "strong" and release strain in high stress drop earthquakes, as indicated in the Vatnafjöll earthquake (Bjarnason and Einarsson, 1991). Seismic risk of small scale structures that are common in the SISZ area (mainly one story buildings) would tend to increase with increased stress-drop for the same size earthquake, since it leads to stronger shaking at high frequencies.

## ACKNOWLEDGMENTS

We thank William Menke, Páll Einarsson, and Dallas Abbott for helpful comments on the manuscript and Páll Einarsson for leading us to the 1912 earthquake rupture sites. We thank Helgi Torfason, Gudrún Larsen, and Bryndís Róbertsdóttir for much valuable geological information. We thank farmers Gudrún Jónsdóttir, Jónína Haflidadóttir, Magnús Runólfsson (1900–1991), and Sigurjón Pálsson for their hospitality and permission to work on their farmlands. This research was supported by the National Science Foundation, the Icelandic National Power Authority (Landsvirkjun), and the Department of Geological Sciences of Columbia University. Lamont-Dohert Contribution 5036.

## REFERENCES

Abe, K. and S. Noguchi (1983). Revision of magnitude of large shallow earthquakes, *Phys. Earth Planet. Interiors* **33,** 1–11.

BAAS (1912). Circulars of the Seismological Committee, British Association for the Advancement of Science, London, No. 26.

Bjarnason, I. Th. and P. Einarsson (1991). Source mechanism of the 1987 Vatnafjöll earthquake in south Iceland, *J. Geophys. Res.* **96,** 4313–4324.

Bjarnason, I. Th., W. Menke, Ó. G. Flóvenz, and D. Caress (1993). Tomographic image of the spreading center in southern Iceland, *J. Geophys. Res.* (in press).

Cowie, P. C. and C. H. Scholz (1992). Growth of faults by accumulation of seismic slip, *J. Geophys. Res.* **97,** 11,085–11,095.

Cox, S. J. D. and C. H. Scholz (1988). On the formation and growth of faults: an experimental study, *J. Struct. Geol.* **10,** 413–430.

Einarsson, P. (1991). Earthquakes and present-day tectonism in Iceland. *Tectonophysics* **189,** 261–279.

Einarsson, P. (1985). Jardskjálftaspár (Earthquake prediction, in Icelandic with an English abstract), *Náttúrufræðingurinn* **55,** 9–28.

Einarsson, P. (1986). Seismicity along the eastern margin of the North American Plate, in *The Geology of North America*, Vol. M, The Western North Atlantic Region, P. R. Vogt and B. E. Tucholke (Editors), Geological Society of America, 99–116.

Einarsson, P., S. Björnsson, G. Foulger, R. Stefánsson, and Th. Skaftadóttir (1981). Seismicity pattern in the South Iceland Seismic Zone, in *Earthquake Prediction: An International Review* D. Simpson and P. G. Richards (Editors), American Geophysical Union, Washington, D.C., 141–151.

Einarsson, P. and J. Eiríksson (1982). Earthquake fractures in the districts Land and Rangárvellir in the South Iceland Seismic Zone, *Jökull* **32,** 113–120.

Einarsson, P. and K. Sæmundsson (1987). Earthquake epicenters 1982–1985 and volcanic systems in Iceland (map), in *"Í hlutarins edli", Festschrift for Thorbjörn Sigurgeirsson*, T. Sigfússon (Editor), Menningarsjódur, Reykjavík.

Goodstein, J. R., H. Kanamori, and W. H. Lee (Editors) (1980). Seimology microfiche publications from the Caltech archives, *Bull. Seism. Soc. Am.* **70,** 657–658.

Gutenberg, B. and C. F. Richter (1954). *Seismicity of the Earth and Associated Phenomena*, 2nd ed., Princeton University Press, Princeton, New Jersey.

Hackman, M. C., G. C. P. King, and R. Bilham (1990). The mechanics of the South Iceland Seismic Zone, *J. Geophys. Res.* **95,** 17339–17351.

Halldórsson, P., R. Stefánsson, P. Einarsson, and S. Björnsson (1984). Mat á jardskjálftahættu: Dysnes, Geldinganes, Helguvík, Vatnsleysuvík, Vogastapi og Thorlákshöfn, Stadarvalsnefnd um idnrekstur, Idnadarrádu-neytid, Reykjavík, 34 pp. (Estimate of seismic hazard, in Icelandic).

Hanks, T. C. and H. Kanamori (1979). A moment magnitude scale, *J. Geophys. Res.* **84,** 2348–2350.

Hjartarson, Á. (1988). Thjórsárhraunid mikla-stærsta nútímahraun jardar, *Náttúrufræðingurinn* **58,** 1–16 (in Icelandic).

Jackson, M. D., E. T. Endo, P. T. Delaney, Th. Arnadottir, and A. M. Rubin (1992). Ground ruptures of the 1974 and 1983 Kaoiki earthquakes, Mauna Loa volcano, Hawaii, *J. Geophys. Res.* **97,** 8775–8796.

Jóhannesson, H. (1980). Stratigraphy and evolution of rift zones, western Iceland, *Náttúrufræðingurinn* **50,** 13–31 (in Icelandic).

Jóhannesson, H., S. P. Jakobsson, and K. Sæmundsson (1990). Geological map of Iceland, sheet 6, S-Iceland, 3rd ed., Icelandic Museum of Natural History and Iceland Geodetic Survey, Reykjavík.

Kárnik, V. (1969). *Seismicity of the European Area 1*, Reidel, Dordrecht, Holland.

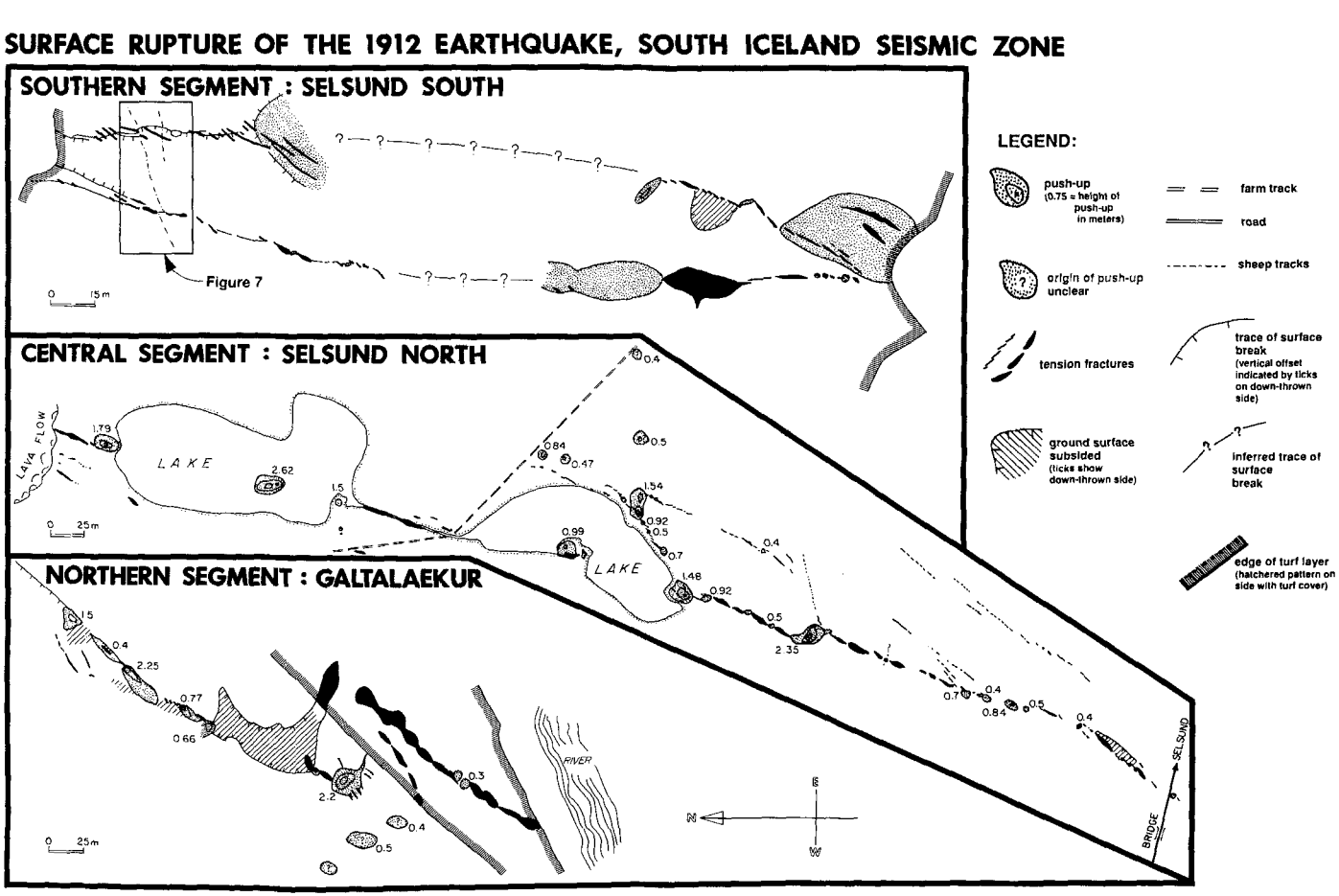


FIG. A1. The complete maps of three selected parts of the surface rupture of the 1912 earthquake. The geographic locations of the mapped areas are shown in Figure 3. All maps are correctly oriented with respect to north as indicated.

Lawn, B. R. and T. R. Wilshaw (1975). *Fracture of Brittle Solids*, Cambridge University Press, Cambridge, 204 pp.

Morgan, W. J. (1981). Hotspot tracks and the opening of the Atlantic and Indian Oceans, *The Sea, Vol. 7, The Oceanic Lithosphere*, C. Emiliani (Editor), Wiley, New York, 443–488.

Olsson, I. U., A. Stenberg, and Y. Goksu (1967). Uppsala natural radiocarbon measurements, *Radiocarbon*, **9,** 454–470.

Óskarsson, N., S. Steinthórsson, and G. E. Sigvaldason (1985). Iceland geocchemical anomaly: origin, volcanotectonics, chemical fractionation and isotope evolution of the crust, *J. Geophys. Res.* **90,** 10,011–10,025.

Paterson, M. S. (1978). *Experimental Rock Deformation: The Brittle Field*, Springer-Verlag, Berlin.

Pálmason, G. and K. Sæmundsson (1974). Iceland in relation the the Mid-Atlantic Ridge, *Ann. Rev. Earth Planet. Sci.* **2,** 25–50.

Scholz, C. H. (1989). Mechanics of faulting, *Ann. Rev. Earth Planet. Sci.* **17,** 309–334.

Scholz, C. H., C. A. Aviles, and S. G. Wesnousky (1986). Scaling differences between large interplate and intraplate earthquakes, *Bull. Seism. Soc. Am.* **76,** 65–70.

Segall, P. and D. D. Pollard (1980). Nucleation and growth of strike slip faults in granite, *J. Geophys. Res.* **88,** 555–568.

Sæmundsson, K. (1974). Evolution of the axial rifting zone in northern Iceland and the Tjörnes fracture zone, *Geol. Soc. Am. Bull.* **85,** 459–504.

Sæmundsson, K. (1979). Outline of the geology of Iceland, *Jökull* **29,** 7–28.

Stefánsson, R. (1967). Some problems of seismological studies on the mid-Atlantic ridge, in *Iceland and Mid-Ocean Ridges*, S. Björnsson (Editor), Societas Scientiarum Islandica, Reykjavík, 80–90.

Thórarinsson, S. (1967). *The Eruptions of Hekla in Historical Times*, Icelandic Scientific Society, Reykjavík, 183 pp.

Tsuneiski, Y., T. Ito, and K. Kano (1978). Surface faulting associated with the 1978 Izu-Oshima-kinkai earthquake, *Bull. Earthq. Res. Inst.* **53,** 649–674.

Vanek, J. A., V. Zapotek, V. Karnick, N. V. Kondorskaya, V. Yu, E. F. Rizmichenko, E. F. Savarensky, S. L. Solovyov, and N. V. Shebalin (1962). Standardization of magnitude scales, *Izvestiya Akad. Nauk S.S.S.R., Ser. Geofiz.* **2,** 153–158.

Vink, G. E. (1984). A hotspot model for Iceland and the Voring Plateau, *J. Geophys. Res.* **89,** 9949–9959.

Ward, P. L. (1971). New interpretation of the geology of Iceland, *Geol. Soc. Am. Bull.* **82,** 2991–3012.

## Appendix A: Surface Rupture of the 1912 Earthquake

Figure A1 shows the complete maps of three selected parts of the surface rupture of the 1912 earthquake.

## Appendix B: Estimation of the Magnitude of the 1912 Earthquake

Kárnik (1969) in his catalog gives a surface-wave magnitude of $M_S = 7.0$ for this event, citing Gutenberg and Richter (1954). We have examined Gutenbergs notepad 78:740 (Goodstein *et al.*, 1980), which gives 14 single-station magnitudes ranging from 6.6 to 7.3 with a mean of 7.0. We have also examined seismic bulletins for six stations in Europe and North America that record surface-wave ground displacements and periods. We obtain a magnitude range from 6.6 to 7.5 with a mean of $M_S = 7.0$, using Vanek *et al.*'s (1962) magnitude formula. Circular 26 of the British Association for the Advancement of Science (BASS, 1912) gives data from 26 Milne instruments operated worldwide. Using these peak trace amplitude measurements, together with Abe and Noguchi's (1983) Milne magnitude formula, we also obtain $M_S = 7.0 \pm 0.1$ (95% confidence).

Lamont-Doherty Earth Observatory
Columbia University
Palisades, New York 10964
(I.Th.B., P.C., M.H.A, L.S., C.H.S.)

Department of Earth Sciences
Columbia University
Palisades, New York 10964
(I.Th.B., P.C., M.H.A., C.H.S.)

Manuscript received 8 June 1992